

BEST AVAILABLE COPY

BEST AVAILABLE COPY

Exhibit A

# Identification of the platelet ADP receptor targeted by antithrombotic drugs

Gunther Hollopeter\*, Hans-Michael Jantzen†, Diana Vincent†, Georgia Litt†, Laura England\*‡, Vanitha Ramakrishnan†, Ruey-Bing Yang†, Paquita Norden§, Alan Norden§, David Julius\* & Pamela B. Conley\*

\* Department of Cellular and Molecular Pharmacology and Program in Neuroscience, University of California, San Francisco, San Francisco, California 94143, USA

† COR Therapeutics, Inc., South San Francisco, California 94080, USA

‡ UMR 5533 CNRS, Hôpital Cardiologique, 33605 Pessac, France

Platelets have a crucial role in the maintenance of normal haemostasis, and perturbations of this system can lead to pathological thrombus formation and vascular occlusion, resulting in stroke, myocardial infarction and unstable angina. ADP released from damaged vessels and red blood cells induces platelet aggregation through activation of the integrin GPIIb-IIIa and subsequent binding of fibrinogen. ADP is also secreted from platelets on activation, providing positive feedback that potentiates the actions of many platelet activators<sup>1</sup>. ADP mediates platelet aggregation through its action on two G-protein-coupled receptor subtypes<sup>2,3</sup>. The P2Y<sub>1</sub> receptor couples to G<sub>q</sub> and mobilizes intracellular calcium ions to mediate platelet shape change and aggregation<sup>4,5</sup>. The second ADP receptor required for aggregation (variously called P2Y<sub>ADP</sub>, P2Y<sub>AC</sub>, P2Y<sub>cyc</sub> or P2T<sub>AC</sub>) is coupled to the inhibition of adenylyl cyclase through G<sub>i</sub>. The molecular identity of the G<sub>i</sub>-linked receptor is still elusive, even though it is the target of efficacious antithrombotic agents, such as ticlopidine and clopidogrel<sup>6–8</sup> and AR-C66096 (ref. 9). Here we describe the cloning of this receptor, designated P2Y<sub>12</sub>, and provide evidence that a patient with a bleeding disorder<sup>10</sup> has a defect in this gene. Cloning of the P2Y<sub>12</sub> receptor should facilitate the development of better antiplatelet agents to treat cardiovascular diseases.

To identify the G<sub>i</sub>-linked platelet ADP receptor, we engineered *Xenopus* oocytes to allow the detection of G<sub>i</sub>-linked responses through a sensitive electrophysiological assay. This strategy is based on the fact that several G<sub>i</sub>-coupled receptors, such as the M2 muscarinic receptor, release Gβγ subunits from heterotrimeric G proteins, thereby activating inwardly rectifying K<sup>+</sup> channels (Kir3.1–3.4)<sup>11</sup>. A complementary DNA library from rat platelets was screened in oocytes expressing Kir3.1 and 3.4, and three positive pools that responded to 10 μM ADP (as determined by an increase in K<sup>+</sup> current) were identified. Subfractionation of one of these pools led to the identification of a single clone tentatively designated as P2Y<sub>12</sub>. The current induced by ADP was K<sup>+</sup>-dependent because replacement of K<sup>+</sup> in the bath solution resulted in a complete loss of current (Fig. 1a). Additionally, injection of Kir or P2Y<sub>12</sub> in vitro RNA transcripts (cRNAs) alone gave no ADP-dependent currents, indicating that the observed signal was not due to activation of an endogenous purinergic receptor and was Kir-dependent (Fig. 1b). Moreover, when cRNA encoding pertussis toxin was injected together with the rat P2Y<sub>12</sub> clone, the response to ADP was abolished (Fig. 1b), as predicted for the G<sub>i</sub>-linked platelet ADP receptor<sup>12</sup>. The human P2Y<sub>12</sub> homologue was isolated from a human platelet library and similar results were obtained when this cRNA was expressed in *Xenopus* oocytes (Fig. 1a, b).

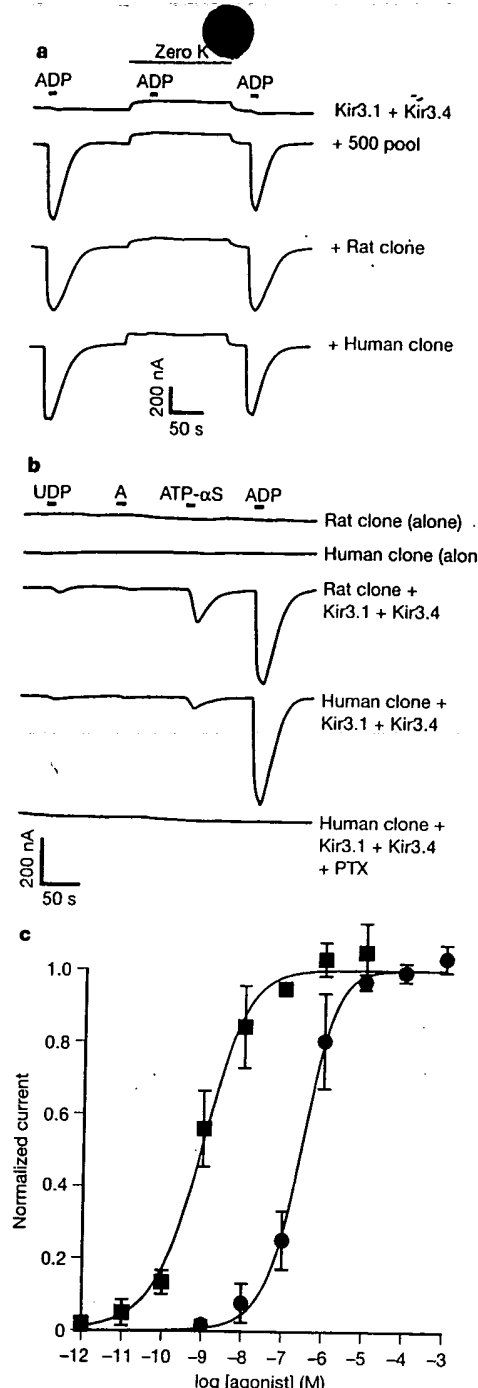


**Figure 1** P2Y<sub>12</sub> is a G-protein-coupled receptor that responds to ADP. **a**, Activation of potassium-dependent currents in *Xenopus* oocytes expressing P2Y<sub>12</sub> with Kir3.1 and 3.4. ADP (10 μM) was applied (short bars) in the presence or absence (long bar) of extracellular potassium (70 mM) while recording membrane currents in the whole-cell voltage-clamp configuration. Oocytes injected with cRNA for Kir3.1 and 3.4 alone (top trace) do not exhibit significant currents in response to the application of ADP unless messages from a positive cDNA pool, the isolated rat P2Y<sub>12</sub> cRNA or the human P2Y<sub>12</sub> homologue are included (lower traces). **b**, ADP-selective stimulation of potassium channel-dependent currents by P2Y<sub>12</sub> occurs via a pertussis-toxin-sensitive pathway. UDP, adenosine (A), ATP-αS or ADP (10 μM each) were sequentially applied to oocytes expressing the rat or human receptor with or without Kir3.1, 3.4 and pertussis toxin (PTX). **c**, The agonist profile of P2Y<sub>12</sub> recapitulates that observed for the G<sub>i</sub>-coupled platelet ADP receptor. Concentration-response curves for ADP (circles) and 2MeSADP (squares) are presented. Membrane currents were normalized in each oocyte to a response obtained with 10 μM ADP. Each point represents the mean (± s.d.) from five independent oocytes. The Hill equation was used to fit the response data.

† Present addresses: Advanced Medicine, South San Francisco, California 94080, USA (G.L.); FibroGen, South San Francisco, California 94080, USA (L.E.).

One hallmark of the G<sub>i</sub>-linked platelet ADP receptor is that substitution of alkylthio groups at the 2-position of the adenine ring increases potency at the receptor<sup>1,13,14</sup>. Consistent with this, 2-methylthioadenosine 5'-diphosphate (2MeSADP) displayed two orders of magnitude more potency than ADP (with half-maximal responses at 0.9 and 300 nM, respectively) (Fig. 1c). In contrast,

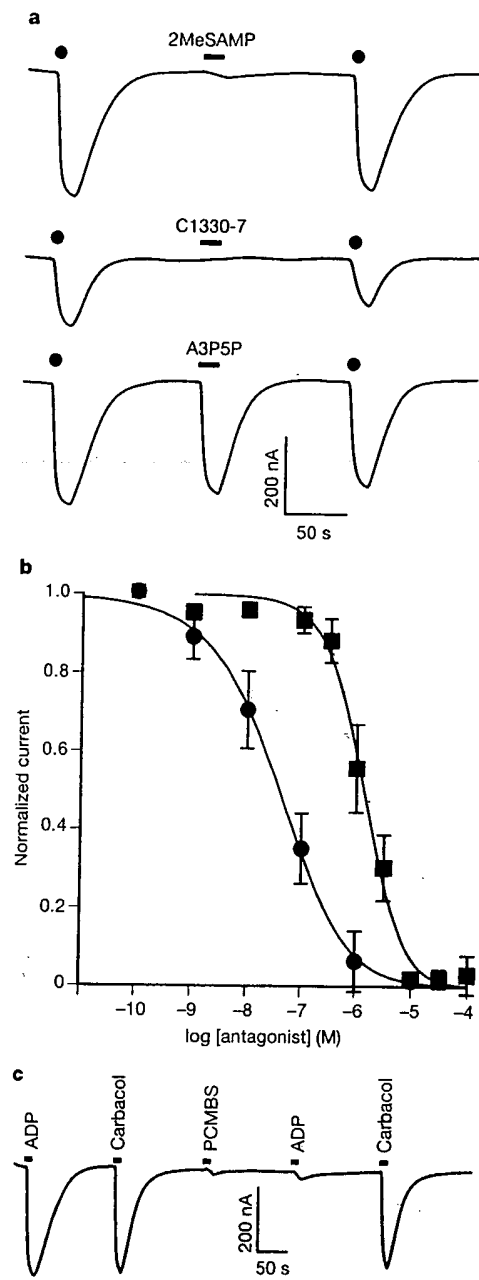


**Figure 2** Currents stimulated by ADP in oocytes expressing hP2Y<sub>12</sub> with Kir3.1 and 3.4 are inhibited by 2MeSAMP, C1330-7 or a thiol reagent. **a**, Current tracing showing reversible blocking of ADP (1  $\mu$ M) responses by 2MeSAMP (10  $\mu$ M) or C1330-7 (1  $\mu$ M), but not by A3P5P (300  $\mu$ M). The dots indicate the start of 15-s applications of ADP; bars indicate co-application with the antagonist. **b**, 2MeSAMP (squares) and C1330-7 (circles) inhibition curves. Current responses were normalized to that elicited by ADP (500 nM) alone in each oocyte and plotted as means  $\pm$  s.d. Curves were fitted to the data with the Hill equation ( $n = 5$  independent oocytes for each point). **c**, Selective ablation of P2Y<sub>12</sub> but not M2 muscarinic receptor signalling by the thiol reagent pCMBS. ADP (10  $\mu$ M), carbachol (1  $\mu$ M) and pCMBS (1 mM) were applied sequentially to an oocyte expressing both receptors concurrently with Kir3.1 and 3.4. Bars indicate periods of drug application (10 s).

other nucleoside or nucleotide derivatives had no effect (Fig. 1b). We also examined the actions of several antagonists specific for the platelet G<sub>i</sub>-linked ADP receptor. Treatment of *Xenopus* oocytes expressing the rat or human P2Y<sub>12</sub> receptor with the nucleotide derivative 2-methylthioadenosine 5'-monophosphate (2MeSAMP)<sup>2</sup> or a non-nucleotide inhibitor C1330-7 (ref. 15) blocked ADP-induced K<sup>+</sup> currents with half-maximal inhibitory concentrations of 1.4  $\mu$ M and 40 nM, respectively (Fig. 2b). In contrast, the P2Y<sub>1</sub>-selective antagonist A3P5P (ref. 16) had no inhibitory effect on the signal evoked by ADP at the rat or human P2Y<sub>12</sub> (Fig. 2a). Thus, when expressed in *Xenopus* oocytes, the P2Y<sub>12</sub> receptor recapitulates the pharmacological profile previously described for the platelet G<sub>i</sub>-linked ADP receptor. The only anomaly that we observed relates to the action of ATP- $\alpha$ S, which behaved as a weak agonist rather than as an antagonist at the cloned receptor. This finding was somewhat unexpected because ATP derivatives reportedly antagonize the platelet G<sub>i</sub>-linked receptor. However, this discrepancy might reflect partial degradation or impurities in commercially available preparations of ATP- $\alpha$ S, or differences between the platelet and oocyte environments such as the degree of ectonucleotidase activity. Indeed, recombinant P2Y<sub>1</sub> receptors respond differentially to ATP, depending on the expression system used<sup>17,18</sup>.

Chinese hamster ovary (CHO) cells expressing the hP2Y<sub>12</sub> receptor displayed ADP-mediated repression of forskolin-stimulated cyclic AMP (cAMP) levels in a dose-dependent manner, reaching a maximum of 47% reduction at 10  $\mu$ M ADP (Fig. 3a). The

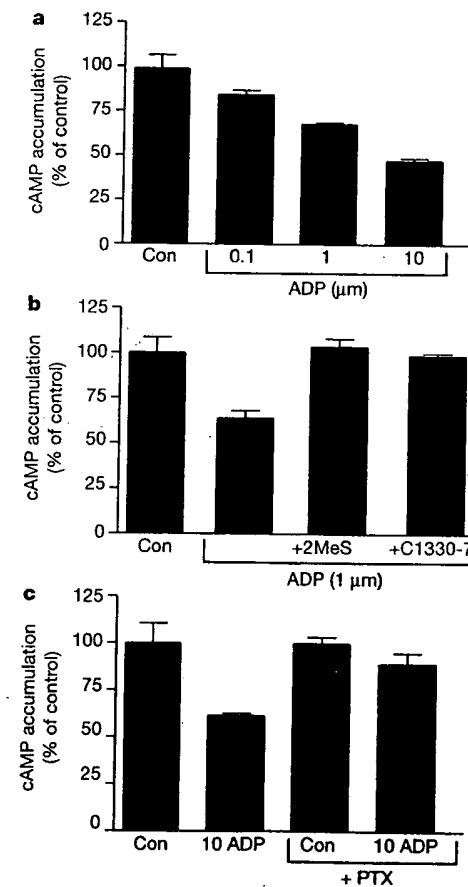


**Figure 3** Activation of hP2Y<sub>12</sub> in CHO cells inhibits adenylyl cyclase. **a**, Receptor coupling to adenylyl cyclase was assessed as ADP-mediated (0.1–10  $\mu$ M) inhibition of forskolin-stimulated (10  $\mu$ M) cAMP accumulation (Con, control; normalized to 100%). **b**, Effect of the specific antagonists 2MeSAMP (2MES) (50  $\mu$ M) and C1330-7 (50  $\mu$ M) on repression of ADP-mediated (1  $\mu$ M) forskolin-stimulated cAMP levels. **c**, Effect of pretreatment with PTX on the inhibition by 10  $\mu$ M ADP of forskolin-stimulated cAMP levels. Results are means  $\pm$  s.d. of three representative experiments performed in triplicate.

repression of cAMP levels by 1  $\mu$ M ADP was reversed by the selective antagonists 2MeSAMP and C1330-7 (Fig. 3b), in agreement with the pharmacological profile observed in *Xenopus* oocytes, and as described for the G<sub>i</sub>-coupled receptor on platelets. Neither of these antagonists had effects on forskolin-stimulated cAMP levels in the absence of agonist. Similar responses to ADP were observed in rat 2-9 fibroblasts stably expressing rP2Y<sub>12</sub> (data not shown). Pretreatment of transfected cells with pertussis toxin abolished effects of ADP on forskolin-stimulated cAMP (Fig. 3c), indicating

that the response is G<sub>i</sub>-mediated.

Northern blot analysis demonstrated that P2Y<sub>12</sub> is abundantly expressed in human platelets, and to a smaller extent in brain (Fig. 4a, b). The predominant transcript of 2.4 kb was absent from all other tissues examined, including peripheral-blood leukocytes. A fainter species of ~4.5 kb was also detected in platelet and brain, whereas a prominent band of ~1.0 kb (Fig. 4b) was observed only in platelet RNA. We also found selective expression in platelets and brain in rat tissues (data not shown). Thus, the mRNA for this novel G-protein-coupled receptor (GPCR) has a restricted expression pattern and is abundantly present in platelets, which is consistent with this cDNA encoding the platelet G<sub>i</sub>-linked receptor. Within the brain, the 2.4-kb species was observed in numerous subregions, including the amygdala, caudate nucleus, corpus callosum, hippocampus, substantia nigra and thalamus (data not shown). Cellular resolution of the expression of rP2Y<sub>12</sub> was obtained by *in situ* hybridization histochemistry of brain sections; punctate staining was noted throughout white and grey matter (Fig. 4c). Principal cells of the hippocampus were not stained, nor was a laminar pattern of expression observed in the neocortex. These observations are consistent with a glial expression pattern. Interestingly, the only cell line previously described to express a P2Y purinergic receptor that is negatively coupled to adenylyl cyclase is the rat C6 glioma cell line<sup>19</sup>. Indeed, we detected a 2.4-kb mRNA species in these cells by northern blot analysis with a rP2Y<sub>12</sub> probe (data not shown).

By using a rabbit polyclonal antiserum directed against the predicted amino terminus of rP2Y<sub>12</sub>, we assessed the surface expression of receptor protein on stably transfected rat 2-9 fibroblasts or rat platelets by flow cytometry. At an antibody concentration of 25  $\mu$ g ml<sup>-1</sup>, ninefold (Fig. 4e) and fourfold (Fig. 4d) increases in mean fluorescence intensity (compared with a control antibody) were observed with transfected cells and platelets, respectively, demonstrating that P2Y<sub>12</sub> protein is indeed expressed on the platelet surface.

When the chromosomal localization of the P2Y<sub>12</sub> gene was determined with the Stanford G3 panel<sup>20</sup> (Research Genetics), P2Y<sub>12</sub>-specific primers mapped closest to STS-D13626, corresponding to the KIAA0001 gene recently identified as a UDP-glucose GPCR<sup>21</sup>. Both of these genes reside on chromosome 3q24–25, interval D3S1279–1280, a region that also includes the human P2Y<sub>1</sub> gene (GeneMap 99; <http://www.ncbi.nlm.nih.gov>). Thus, this interval contains genes encoding at least three receptors, two of which (P2Y<sub>1</sub> and P2Y<sub>12</sub>) mediate ADP-dependent platelet aggregation. Among GPCRs, P2Y<sub>12</sub> is most closely related to the UDP-glucose receptor<sup>21</sup> (44% identical) but much less so to P2Y<sub>1</sub> (19% identical), suggesting that the UDP-glucose and P2Y<sub>12</sub> receptors are the products of a relatively recent gene duplication on chromosome 3.

The predicted hP2Y<sub>12</sub> protein contains four extracellular cysteine residues (see Fig. 5). A critical role of cysteine residues in the function of the platelet ADP receptor has been suggested by the ability of thiol reagents to ablate ADP responses in platelets<sup>1</sup>. Indeed, the antithrombotic agent clopidogrel is proposed to inactivate the G<sub>i</sub>-linked platelet ADP receptor through a mechanism in which it is metabolized to a thiol species that modifies a cysteine residue on the receptor<sup>22</sup>. We found that a brief exposure of oocytes expressing Kir3.1, 3.4 and hP2Y<sub>12</sub> to the thiol reagent p-chloromercuriphenylsulphonic acid (pCMBS) eliminated ADP-evoked current responses (Fig. 2c). Inhibition was selective for the P2Y<sub>12</sub> receptor because the activation of this signalling pathway by M2 muscarinic receptors expressed in the same oocytes was unaffected by treatment with pCMBS.

Nurden *et al.*<sup>10</sup> have previously described a patient (M.L.) with a mild bleeding disorder. Platelets from M.L. exhibit impaired ADP-dependent platelet aggregation, greatly reduced ADP binding activity and lack the ability to inhibit cAMP levels in response to ADP. However, the P2Y<sub>1</sub>-receptor-mediated responses, such as

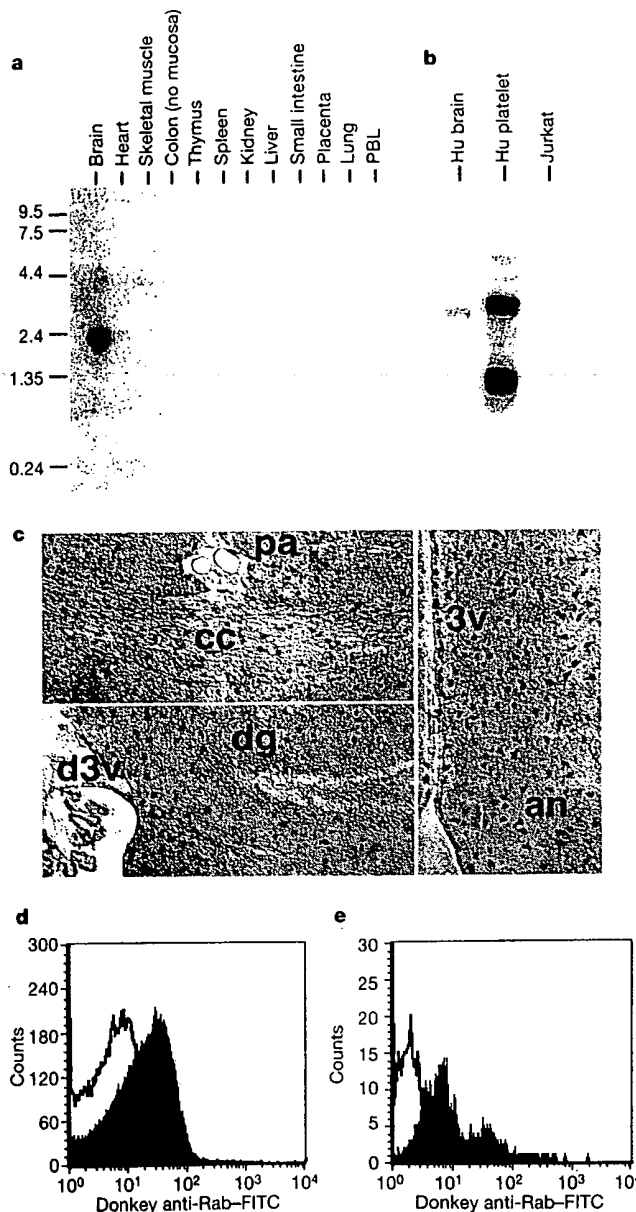


**Figure 4** P2Y<sub>12</sub> receptor is selectively expressed in platelets and brain. **a, b**, Northern analysis of hP2Y<sub>12</sub> transcripts. All lanes contained 2  $\mu$ g poly(A)<sup>+</sup> mRNA except samples from platelet and Jurkat cells, which contain 20  $\mu$ g total RNA. PBL, peripheral blood lymphocytes; Hu, human. Kilobases (kb) are indicated on the left. **c**, rP2Y<sub>12</sub> transcripts are distributed throughout the brain in presumptive glia. Staining was equally abundant in fibre tracts (cc, corpus callosum) and regions enriched for neuronal cell bodies (dg, dentate gyrus; an, arcuate nucleus of the hypothalamus), but was absent from vasculature (pa, pericallosal artery). Control (sense) riboprobes did not stain these regions. Ventricular structures are also indicated (d3v, dorsal third ventricle; 3v, third ventricle). **d**, FACS analysis of rat platelets stained with rP2Y<sub>12</sub> antisera (filled peak) or a control IgG (unfilled peak). Rab, rabbit. **e**, FACS analysis of rat 2-9 fibroblasts transfected with the rP2Y<sub>12</sub> cDNA clone (filled peak) or untransfected rat 2-9 fibroblasts (open peak).

intracellular  $\text{Ca}^{2+}$  ion mobilization and shape change, are not affected, indicating that this patient has a selective defect in the  $G_i$ -linked receptor. Analysis of polymerase chain reaction (PCR) products from the P2Y<sub>12</sub> coding region from M.L.'s genomic DNA revealed the presence of one mutant allele at this locus, as confirmed by direct sequencing of at least three independent PCR reactions. The mutation found in the gene encoding P2Y<sub>12</sub> consists of a deletion of two nucleotides (TTCATT) within the coding region, at amino acid 240 (near the N-terminal end of TM6), thus shifting the reading frame for 28 residues before introducing a premature stop codon (Fig. 5b). This mutation was not detected in 100 randomly chosen, ethnically matched control individuals. Biochemical studies suggest that platelets from M.L. lack  $G_i$ -linked ADP receptors, yet our sequence analysis indicates that this

individual has one mutant and one wild-type P2Y<sub>12</sub> allele, at least in the protein-coding region. This suggests either that the P2Y<sub>12</sub> mutation identified exerts a dominant-negative effect or that M.L. harbours an additional mutation that eliminates the expression of the allele containing a wild-type coding region. We evaluated the former possibility with our electrophysiological assay (Fig. 5c). First, no significant activity was observed when oocytes were injected with cRNA transcripts corresponding to the frame-shifted allele, demonstrating that this mutant is indeed non-functional. Moreover, when mutant and wild-type cRNAs were injected together into oocytes at different ratios, no inhibition of the signal from the wild-type allele was observed, demonstrating that the mutant allele does not act in a dominant-negative manner. Further support for this conclusion comes from sequence analysis of the P2Y<sub>12</sub> coding region from

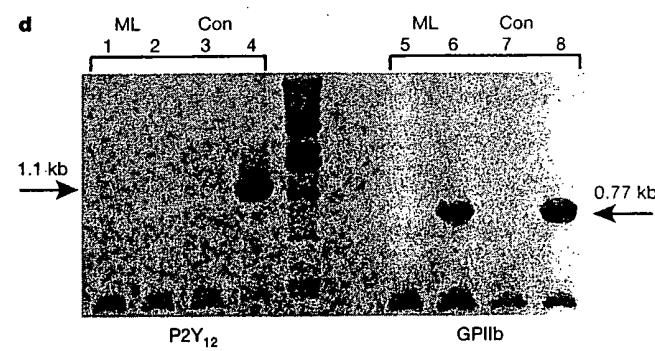
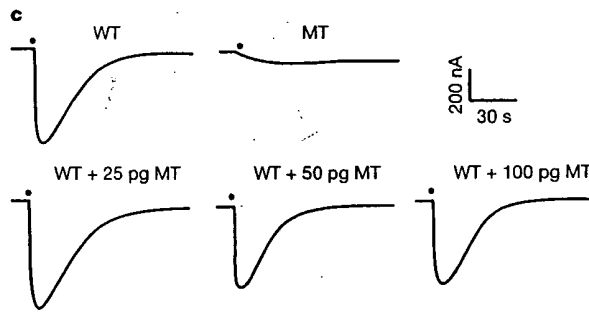
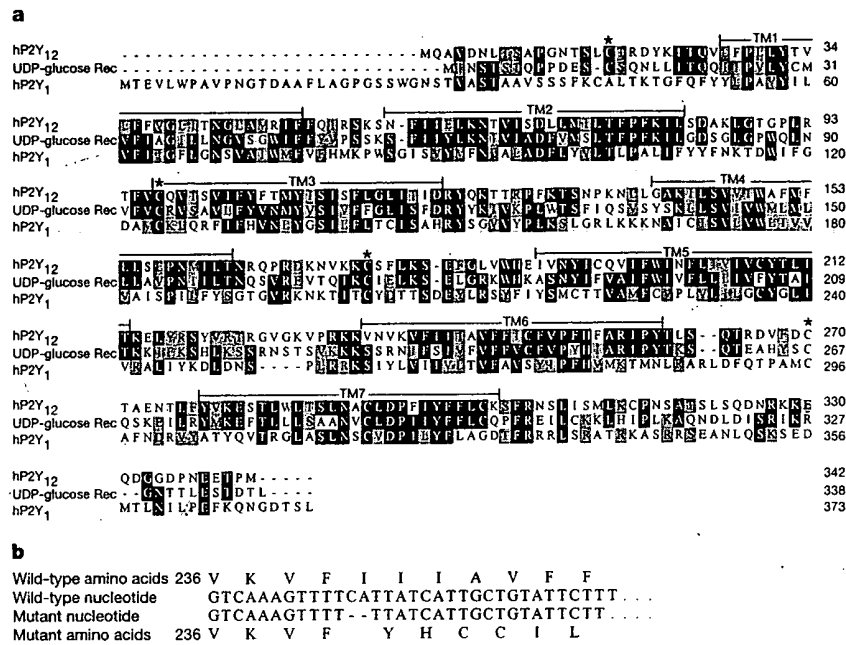


**Figure 5** A frame-shift mutation within the hP2Y<sub>12</sub> gene is associated with a bleeding disorder. **a**, Deduced amino acid sequence of the hP2Y<sub>12</sub> protein and its alignment with other homologous receptor sequences. The putative membrane-spanning domains are designated with bars above the sequence. hP2Y<sub>12</sub> sequence is aligned with the sequences of hP2Y<sub>1</sub> receptor (also expressed in platelets and activated by ADP), as well as with the human UDP-glucose receptor, with which it shares the greatest homology. Shading denotes amino acid identity (black) or similarity (grey); asterisks denote extracellular cysteine residues. **b**, A P2Y<sub>12</sub> allele from a patient (M.L.) with defective ADP-dependent aggregation contains a 2-base-pair deletion, resulting in a frame-shift mutation and a premature truncation of the protein. **c**, Mutant hP2Y<sub>12</sub> receptor from patient M.L. is non-functional and does not act in a dominant-negative capacity. Representative ADP-evoked membrane currents from an oocyte injected with 50 pg wild-type (WT) hP2Y<sub>12</sub> cRNA (upper left panel), 50 pg mutant (MT) hP2Y<sub>12</sub> cRNA (upper right panel) or with 50 pg WT and increasing amounts of MT hP2Y<sub>12</sub> cRNAs (bottom panels). Oocytes were also injected with 1 ng Kir3.1 and 1 ng Kir3.4 cRNAs. Dots indicate the onset of ADP application (10  $\mu\text{M}$  for 5 s). **d**, Patient M.L. has abnormally low levels of RT-PCR product derived from P2Y<sub>12</sub> mRNA. RT-PCR with primers specific for either P2Y<sub>12</sub> (lanes 1–4) or GPIIb (lanes 5–8) was performed with whole-blood RNA from patient M.L. (lanes 1, 2, 5 and 6) or a control (Con) sample (lanes 3, 4, 7 and 8). PCR reactions were performed on RNA samples without reverse transcriptase to control for genomic DNA contamination (lanes 1, 3, 5 and 7). A 1.1-kb product encoding the P2Y<sub>12</sub> open reading frame was amplified from the control sample but was virtually absent from M.L. (a faint product could be observed after longer exposure). In contrast, the amount of product (0.77 kb) amplified from GPIIb mRNA was equivalent between M.L. and control. Sequence analysis reveals that M.L.'s P2Y<sub>12</sub> RT-PCR product was derived solely from the mutant allele.

panel) or with 50 pg WT and increasing amounts of MT hP2Y<sub>12</sub> cRNAs (bottom panels). Oocytes were also injected with 1 ng Kir3.1 and 1 ng Kir3.4 cRNAs. Dots indicate the onset of ADP application (10  $\mu\text{M}$  for 5 s). **d**, Patient M.L. has abnormally low levels of RT-PCR product derived from P2Y<sub>12</sub> mRNA. RT-PCR with primers specific for either P2Y<sub>12</sub> (lanes 1–4) or GPIIb (lanes 5–8) was performed with whole-blood RNA from patient M.L. (lanes 1, 2, 5 and 6) or a control (Con) sample (lanes 3, 4, 7 and 8). PCR reactions were performed on RNA samples without reverse transcriptase to control for genomic DNA contamination (lanes 1, 3, 5 and 7). A 1.1-kb product encoding the P2Y<sub>12</sub> open reading frame was amplified from the control sample but was virtually absent from M.L. (a faint product could be observed after longer exposure). In contrast, the amount of product (0.77 kb) amplified from GPIIb mRNA was equivalent between M.L. and control. Sequence analysis reveals that M.L.'s P2Y<sub>12</sub> RT-PCR product was derived solely from the mutant allele.

M.L.'s daughter, who has previously been shown to have an intermediate number of ADP-binding sites and impaired ADP-dependent aggregation<sup>10</sup>. Like her father, she has one wild-type and one frame-shifted allele, and is therefore likely to be a true heterozygote, both phenotypically and genetically. If so, then the truncated receptor does not act as a dominant-negative *in vivo*. Finally, we asked whether M.L.'s alleles are both expressed by performing a PCR analysis after reverse transcription (RT-PCR) of RNA from his platelets. Extremely low levels of P2Y<sub>12</sub>-derived product were obtained compared with levels amplified from an unaffected individual or compared with a control transcript encoding platelet GPIIb (Fig. 5D). In addition, a sequence analysis of P2Y<sub>12</sub> RT-PCR products demonstrated that M.L.'s P2Y<sub>12</sub> transcripts are derived from the mutant allele; no wild-type product was detected. We therefore conclude that M.L.'s lack of functional G<sub>i</sub>-coupled platelet ADP receptor activity occurs because he expresses only the frame-shifted allele. The mechanism by which expression of the wild-type allele is repressed is not clear. Other patients with congenital platelet defects have been reported<sup>23</sup>, and it will be interesting to determine whether these are also associated with mutations in P2Y<sub>12</sub>.

We have characterized a novel cDNA from a platelet library that encodes the G<sub>i</sub>-linked platelet ADP receptor. Genetic<sup>4,5,10,23</sup> and pharmacological<sup>24,25</sup> studies demonstrate that the G<sub>i</sub>-linked receptor is critical for the formation and stabilization of large platelet aggregates<sup>26</sup>. Additionally, the G<sub>i</sub>-linked receptor is the target of the antithrombotic drugs clopidogrel and ticlopidine, which have been demonstrated to be effective in treating a variety of thrombotic diseases (stroke, myocardial infarction, peripheral vascular disease). However, these drugs work through a mechanism of covalent protein modification, which might underlie their recent association with the syndrome thrombotic thrombocytopenic purpura<sup>27</sup>, an immune-mediated response. Our studies demonstrate that the P2Y<sub>12</sub> receptor has a selective tissue distribution compared with other purinergic receptors (such as P2Y<sub>1</sub>), making this receptor an extremely attractive target for the development of new anti-thrombotic drugs.

## Methods

### Platelet cDNA library

Poly-A<sup>+</sup> mRNA from rat platelets was used to generate a directional oligo(dT)-primed cDNA library in the pcDNA3.1<sup>+</sup> vector. Roughly 320,000 clones were divided into 48 individual pools. Linearized cDNA templates from these pools were transcribed *in vitro* with T7 RNA polymerase (Ambion). Sib selection of a positive pool was performed to subfractionate the signal to the level of 96 clones. All were sequenced and a novel GPCR was further characterized. Rat P2Y<sub>12</sub> cDNA (GenBank accession number AF313450) was used to isolate a human orthologue from a platelet λ ZAP cDNA library. A full-length hP2Y<sub>12</sub> cDNA expression construct was obtained by ligation of a λ clone and a fragment derived by 3' rapid amplification of cloned ends into the pcneo expression vector (Promega). The GenBank accession number for human P2Y<sub>12</sub> is AF313449.

### Platelet RT-PCR

Informed consent was obtained from M.L. and his daughter for the purposes of this study. Whole blood (30 ml) was lysed and total RNA was isolated with TriReagent BD (Molecular Research Center). First-strand cDNA was generated (Superscript 2, Life Technologies) and PCR (35 cycles) was performed with the following mRNA-specific primers. The P2Y<sub>12</sub> primers 5' (5'-CCAGAACACAGTTATCAGTAACC-3') and 3' (5'-GTCAGTTAATATTTTACTTAGCGCTTGC-3') were annealed at 57°C, whereas the GPIIb primers 5' (5'-GTCACGGGGATGGGAGGCATGA-3') and 3' (5'-GTCTGCCCTCATCTCGAAGGAAGG-3') were annealed at 60°C. PCR products were analysed by electrophoresis in 1% agarose, and bands of the correct size were isolated for direct sequencing.

### Electrophysiology

Defolliculated *Xenopus laevis* oocytes were injected with a positive 500 clone pool (10 ng), rP2Y<sub>12</sub> (10 pg), hP2Y<sub>12</sub> (50 pg), Kir3.1, Kir3.4, PTX or hM2 (1 ng each) cRNAs as indicated. Three to seven days after injection, two-electrode voltage-clamp recordings were performed with a Geneclamp 500 amplifier (Axon Instruments) and a Maclab analogue-to-digital converter (Maclab). Membrane potentials were clamped at -70 mV while the recording chamber was perfused at a rate of 2 ml min<sup>-1</sup> with a solution containing (in mM) 70 KCl, 20 NaCl, 3 MgCl<sub>2</sub>, 5 HEPES, pH 7.4, at room temperature. The KCl was replaced with NaCl to examine responses in the absence of potassium. Agonists and antagonists (Roche Molecular Biochemistry or Sigma) were diluted in the

recording solution. Experiments with hP2Y<sub>12</sub> included 0.1% dimethyl sulphoxide to enhance its solubility in the perfusate.

### Generation of stable mammalian cell lines and cAMP assays

Chinese hamster ovary cells or rat 2-9 fibroblasts, which are null for G<sub>i</sub>-linked purinergic receptors, were transfected with hP2Y<sub>12</sub> or rP2Y<sub>12</sub> cDNAs, respectively, with FuGene reagent (Roche), and cells were cultured in the presence of G418 for 2 weeks to select for stable transfectants. For cAMP assays, stably transfected CHO cells expressing the hP2Y<sub>12</sub> plasmid were plated in 12-well dishes. After 48 h, medium was removed from the cells and replaced with serum-free medium containing IBMX (0.25 mM final) and incubated at 37°C for 5 min. Cells were incubated for an additional 5 min with 10 μM forskolin, as well as the indicated agonists and antagonists. Pertussis toxin treatment (30 ng/ml) occurred for 20 h at 37°C before assay. Levels of cAMP were determined from aliquots of cell extracts in a radioimmunoassay (Amersham Biotrak cAMP <sup>125</sup>I assay system).

### Northern and *In situ* hybridizations

Northern blots of poly(A)<sup>+</sup> RNA from human tissues (Clontech) or total human platelet RNA was hybridized with radiolabelled hP2Y<sub>12</sub> cDNA fragments under standard conditions. Digoxigenin-labelled *In situ* hybridization was performed on coronal rat brain sections by using an RNA probe corresponding to the antisense sequence of rP2Y<sub>12</sub> (ref. 28).

### Flow cytometry

Adult male Sprague-Dawley rats were anaesthetized and whole blood was isolated; citrate was used as anticoagulant. Platelet-rich plasma was isolated by centrifugation and used for flow-cytometry analysis. A rabbit anti-serum (SynPep Corporation) was produced to the N-terminal 23 residues of rP2Y<sub>12</sub>. IgG was purified with protein G-Sepharose. Rat platelet-rich plasma (2 × 10<sup>6</sup> cells) and cultured rat 2-9 fibroblasts transfected with rP2Y<sub>12</sub> cDNA (10<sup>5</sup> cells) were incubated with purified IgG (10–50 μg/ml) in FACS buffer (phosphate-buffered saline containing 0.1% BSA and 2% heat-inactivated fetal bovine serum) in a total volume of 100 μl for 1 h at 4°C. Cells and platelets were then washed with cold FACS buffer and incubated with 2.5 μg ml<sup>-1</sup> FITC-conjugated goat anti-rabbit antibody for 30 min at 4°C. Cells and platelets were washed, resuspended in cold FACS buffer, and fluorescence of cell-bound secondary antibody was determined with a FACSort flow cytometer (Becton-Dickinson). Control samples contained cells without antibodies (for the determination of autofluorescence), cells with control rabbit IgG, or secondary antibodies alone.

Received 13 June; accepted 10 October 2000.

1. Mills, D. C. ADP receptors on platelets. *Thromb. Haemost.* 76, 835–856 (1996).
2. Jantzen, H. M. *et al.* Evidence for two distinct G-protein-coupled ADP receptors mediating platelet activation. *Thromb. Haemost.* 81, 111–117 (1999).
3. Daniel, J. L. *et al.* Molecular basis for ADP-induced platelet activation. I. Evidence for three distinct ADP receptors on human platelets. *J. Biol. Chem.* 273, 2024–2029 (1998).
4. Leon, C. *et al.* Defective platelet aggregation and increased resistance to thrombosis in purinergic P2Y<sub>1</sub> receptor-null mice. *J. Clin. Invest.* 104, 1731–1737 (1999).
5. Fabre, J. E. *et al.* Decreased platelet aggregation, increased bleeding time and resistance to thromboembolism in P2Y<sub>1</sub>-deficient mice. *Nature Med.* 5, 1199–1202 (1999).
6. Gachet, C. *et al.* The thienopyridine ticlopidine selectively prevents the inhibitory effects of ADP but not of adrenaline on cAMP levels raised by stimulation of the adenylate cyclase of human platelets by PGE<sub>1</sub>. *Biochem. Pharmacol.* 40, 2683–2687 (1990).
7. Gachet, C. *et al.* ADP receptor induced activation of guanine nucleotide binding proteins in rat platelet membranes—an effect selectively blocked by the thienopyridine clopidogrel. *Thromb. Haemost.* 68, 79–83 (1992).
8. Mills, D. C. B. *et al.* Clopidogrel inhibits the binding of ADP analogues to the receptor mediating inhibition of platelet adenylate cyclase. *Arterioscler. Thromb. 12*, 430–436 (1992).
9. Humphries, R. G., Tomlinson, W., Ingall, A. H., Cage, P. A. & Leff, P. A novel, highly potent and selective antagonist at human platelet P<sub>2</sub>T-purinoreceptors. *Br. J. Pharmacol.* 113, 1057–1063 (1994).
10. Nurden, P. *et al.* An inherited bleeding disorder linked to a defective interaction between ADP and its receptor on platelets. *J. Clin. Invest.* 95, 1612–1622 (1995).
11. Krapivinsky, G., Krapivinsky, L., Wickman, K. & Clapham, D. E. Gα<sub>B</sub> binds directly to the G protein-gated K<sup>+</sup> channel, IK<sub>ACh</sub>. *J. Biol. Chem.* 270, 29059–29062 (1995).
12. Ohlmann, P. *et al.* The human platelet ADP receptor activates G<sub>2</sub> proteins. *Biochem. J.* 312, 775–779 (1995).
13. MacFarlane, D. E., Srivastava, P. C. & Mills, D. C. B. 2-Methylthioadenosine[β-<sup>32</sup>P]diphosphate: an agonist and radioligand for the receptor that inhibits the accumulation of cyclic AMP in intact blood platelets. *J. Clin. Invest.* 71, 420–428 (1983).
14. Hourani, S. M. O. & Hall, D. Receptors for ADP on human blood platelets. *Trends Pharmacol. Sci.* 15, 103–108 (1994).
15. Jantzen, H.-M. *et al.* Evidence for two distinct G protein-coupled ADP receptors mediating platelet activation. *Blood* 92, 303a (1998).
16. Boyer, J. L., Romero-Avila, T., Schachter, J. B. & Harden, T. K. Identification of competitive antagonists of the P2Y<sub>1</sub> receptor. *Mol. Pharmacol.* 50, 1323–1329 (1996).
17. Palmer, R. K., Boyer, J. L., Schachter, J. B., Nicholas, R. A. & Harden, T. K. Agonist action of adenosine triphosphates at the human P2Y<sub>1</sub> receptor. *Mol. Pharmacol.* 54, 1118–1123 (1998).
18. Filippov, A. K., Brown, D. A. & Barnard, E. A. The P2Y<sub>1</sub> receptor closes the N-type Ca<sup>2+</sup> channel in neurones, with both adenosine triphosphates and diphosphates as potent agonists. *Br. J. Pharmacol.* 129, 1063–1066 (2000).
19. Boyer, J. L., Lazarowski, E. R., Chen, X. H. & Harden, T. K. Identification of a P2Y-purinergic receptor that inhibits adenylyl cyclase. *J. Pharmacol. Exp. Ther.* 267, 1140–1146 (1993).
20. Stewart, E. *et al.* An STS-based radiation hybrid map of the human genome. *Genome Res.* 7, 422–433 (1997).

21. Chambers, J. K. et al. A G protein-coupled receptor for UDP-glucose. *J. Biol. Chem.* 275, 10767–10771 (2000).
22. Savi, P. et al. Identification and biological activity of the active metabolite of Clopidogrel. *Thromb. Haemost.* (in press).
23. Cattaneo, M. & Gachet, C. ADP receptors and clinical bleeding disorders. *Arterioscler. Thromb. Vasc. Biol.* 19, 2281–2285 (1999).
24. Jarvis, G. E., Humphries, R. G., Robertson, M. J. & Leff, P. ADP can induce aggregation of human platelets via both P2Y(1) and P(2T) receptors. *Br. J. Pharmacol.* 129, 275–282 (2000).
25. Hechler, B., Eckly, A., Ohlmann, P., Cazenave, J.-P. & Gachet, C. The P2Y receptor, necessary but not sufficient to support full ADP-induced platelet aggregation, is not the target of the drug clopidogrel. *Br. J. Haematol.* 103, 858–866 (1998).
26. Humbert, M. et al. Ultrastructural studies of platelet aggregates from human subjects receiving clopidogrel and from a patient with an inherited defect of an ADP-dependent pathway of platelet activation. *Arterioscler. Thromb. Vasc. Biol.* 16, 1532–1543 (1996).
27. Bennett, C. L. et al. Thrombotic thrombocytopenic purpura associated with clopidogrel. *N. Engl. J. Med.* 325, 1371–1372 (2000).
28. Caterina, M. J. et al. The capsaicin receptor: a heat-activated ion channel in the pain pathway. *Nature* 389, 816–824 (1997).

#### Acknowledgements

We thank E. Peralta for advice and encouragement. We also thank H. Chuang for advice with electrophysiological assays; A. Laiberman and R. Scarborough for C1330-7; P. Castro and L. Komives for assistance and advice with the *in situ* hybridization; the Oksenberg and Reijo laboratories for human DNA samples; E. Thompson, K. Simpson, S. Hollenbach and K. Ministri-Madrid and the COR animal facility for technical assistance; R. Wong and D. De Guzman for assistance with figures; and C. Homcy, E. E. Reynolds, J. Topper and D. Phillips for discussions. D.J. is supported by funding from NIH and NIMH; G.H. is supported by a NIH predoctoral neuroscience training grant.

Correspondence and requests for materials should be addressed to P.B.C.  
(e-mail: pconley@corr.com).

## Inactivation of the apoptosis effector Apaf-1 in malignant melanoma

**Maria S. Soengas\***, Paola Capodieci†, David Polksky†, Jaume Morat†, Manel Esteller†, Ximena Opitz-Araya\*, Richard McCombie\*, James G. Herman‡, William L. Gerald†, Yuri A. Lazebnik\*, Carlos Cordón-Cardó† & Scott W. Lowe\*

\* Cold Spring Harbor Laboratory, Cold Spring Harbor, New York 11724, USA

† Memorial Sloan Kettering Cancer Center, New York, New York 10021, USA

‡ Johns Hopkins Oncology Center and Johns Hopkins University, Baltimore, Maryland 21231, USA

Metastatic melanoma is a deadly cancer that fails to respond to conventional chemotherapy and is poorly understood at the molecular level<sup>1</sup>. *p53* mutations often occur in aggressive and chemoresistant cancers but are rarely observed in melanoma<sup>1,2</sup>. Here we show that metastatic melanomas often lose Apaf-1, a cell-death effector that acts with cytochrome c and caspase-9 to mediate *p53*-dependent apoptosis<sup>3</sup>. Loss of Apaf-1 expression is accompanied by allelic loss in metastatic melanomas, but can be recovered in melanoma cell lines by treatment with the methylation inhibitor 5-aza-2'-deoxycytidine (5aza2dC). Apaf-1-negative melanomas are invariably chemoresistant and are unable to execute a typical apoptotic programme in response to *p53* activation. Restoring physiological levels of Apaf-1 through gene transfer or 5aza2dC treatment markedly enhances chemosensitivity and rescues the apoptotic defects associated with Apaf-1 loss. We conclude that Apaf-1 is inactivated in metastatic melanomas, which leads to defects in the execution of apoptotic cell death. Apaf-1 loss may contribute to the low frequency of *p53* mutations observed in this highly chemoresistant tumour type.

Mutations in the *p53* tumour-suppressor gene are extremely common in most human cancers, and are often associated with poor patient prognosis and treatment failure<sup>4</sup>. *p53* promotes cell-cycle arrest or apoptosis in response to cellular damage, including

that induced by many chemotherapeutic drugs<sup>4</sup>. As a consequence, *p53* loss can promote drug resistance in experimental and clinical settings<sup>4,5</sup>. Caspase-9 (Casp9) and its cofactor Apaf-1 can be essential downstream effectors of *p53* during apoptosis, such that inactivation of either Apaf-1 or Casp9 substitutes for the loss of *p53* in enhancing the transformation potential of primary murine fibroblasts<sup>3</sup>, and in promoting chemoresistance<sup>3,6,7</sup>. Hence, Apaf-1 and Casp9 are potential tumour suppressors that may affect treatment sensitivity.

To investigate whether Apaf-1 is a tumour suppressor, we surveyed several tumour types for loss-of-function mutations in the *Apaf-1* gene. We included melanoma in this analysis because it is extremely resistant to apoptosis-inducing agents but retains wild-type *p53* (ref. 1). We analysed a series of metastatic melanoma samples (see Supplementary Information) for their *p53* and Apaf-1 status. As expected, a low rate of mutation was detected for *p53* in these tumours (see Supplementary Information). In contrast, a markedly high rate of allelic loss was found for polymorphic markers encompassing the *Apaf-1* locus on chromosome 12q23 (> 40%; Fig. 1a and b). Moreover, tumours with loss of heterozygosity (LOH) expressed little *Apaf-1* message by *in situ* hybridization (Fig. 1c, d), compared with tumours with no LOH (Fig. 1c, d).

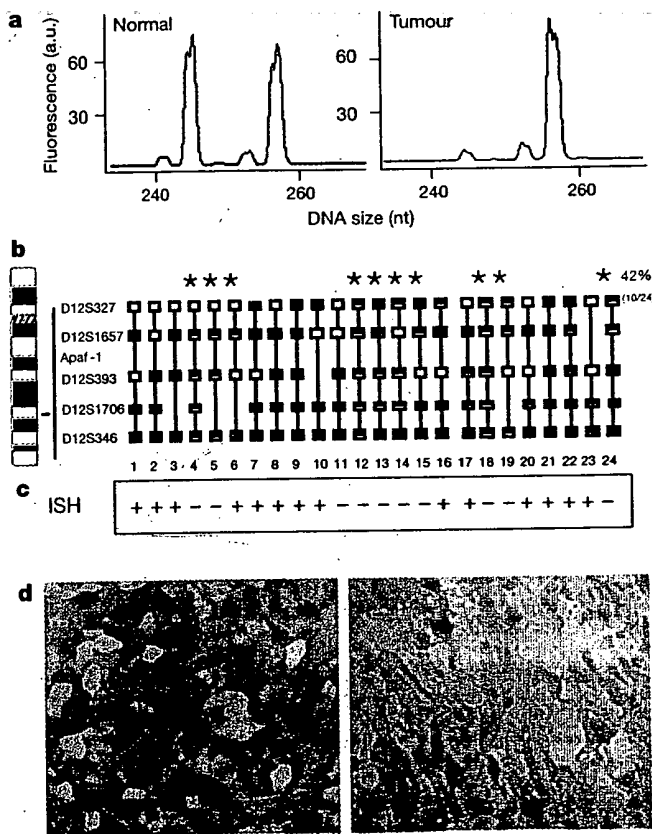


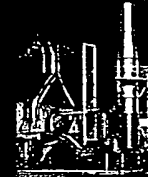
**Figure 1** Apaf-1 loss in metastatic melanoma. **a**, Fluorescent electropherograms for microsatellite marker D12S393 on chromosome 12q22–23. The normal (left) and tumour (right) counterparts of case four are indicated. a.u., arbitrary units. **b**, Summary of LOH analysis for 24 normal/tumour pairs, showing non-informative (homozygous) markers (white), retained markers (blue) and markers with LOH (red). Each vertical line indicates a single patient, and cases having LOH at Apaf-1 flanking markers are indicated with a red asterisk. **c**, Estimation of Apaf-1 messenger RNA levels by *in situ* hybridization using Apaf-1 antisense probe (residues 2,112–2,225). Relative levels are indicated as high (+) and low or undetectable (-). **d**, Representative examples of samples described in c. Left, tumour case 7 (no LOH); right, tumour case 19 (LOH). A 'sense' probe control produced no signal (data not shown). Similar results were obtained for probes targeting other Apaf-1 regions (residues 1–461, 581–1,363 or 3,426–3,710) (data not shown).

# nature

\$10.00

[www.nature.com](http://www.nature.com)

**nature  
insight**  
Biocatalysis



**Biocatalysis**  
Nature Insight

## A chip off the old continent

### **Functional proteomics**

Protein interactions in a  
human pathogen

### **Molecular clouds**

Mapping by starlight

### **Ecology**

Saving the Everglades

**This Page is Inserted by IFW Indexing and Scanning  
Operations and is not part of the Official Record**

**BEST AVAILABLE IMAGES**

Defective images within this document are accurate representations of the original documents submitted by the applicant.

Defects in the images include but are not limited to the items checked:

- BLACK BORDERS**
- IMAGE CUT OFF AT TOP, BOTTOM OR SIDES**
- FADED TEXT OR DRAWING**
- BLURRED OR ILLEGIBLE TEXT OR DRAWING**
- SKEWED/SLANTED IMAGES**
- COLOR OR BLACK AND WHITE PHOTOGRAPHS**
- GRAY SCALE DOCUMENTS**
- LINES OR MARKS ON ORIGINAL DOCUMENT**
- REFERENCE(S) OR EXHIBIT(S) SUBMITTED ARE POOR QUALITY**
- OTHER: \_\_\_\_\_**

**IMAGES ARE BEST AVAILABLE COPY.**

**As rescanning these documents will not correct the image problems checked, please do not report these problems to the IFW Image Problem Mailbox.**